LAB/IN VITRO RESEARCH

e-ISSN 1643-3750
© Med Sci Monit, 2026; 32: e953474
DOI: 10.12659/MSM.953474

Received: 2026.03.18
Accepted: 2026.06.11
Available online: 2026.06.23
Published: 2026.XX.XX

Combination of Astragaloside IV and Tetramethylpyrazine Promotes Angiogenesis via the MALAT1–CXCL12/CXCR4 Axis in Brain Endothelial Cells After Ischemic Injury

Authors' Contribution:
Study Design A
Data Collection B
Statistical Analysis C
Data Interpretation D
Manuscript Preparation E
Literature Search F
Funds Collection G

ABCDEF 1,2 Guangya Li*
AEG 1 Yunwei Lu*
BEF 1 Liuling Huang
BEF 1 Jingwen Zhu
DEF 1 Liling Li
EF 1 Peize Li
EF 1 Shanshan Li
AEG 1 Xiude Qin

1 Department of Neurology and Psychology, The Fourth Clinical Medical College of Guangzhou University of Chinese Medicine (Shenzhen Traditional Chinese Medicine Hospital), Shenzhen, Guangdong, PR China
2 Tianjin University of Traditional Chinese Medicine, Tianjin, PR China

* Guangya Li and Yunwei Lu contributed equally to this paper as co-first authors

Corresponding Author: Xiude Qin, Department of Neurology and Psychology, the Fourth Clinical Medical College of Guangzhou University of Chinese Medicine (Shenzhen Traditional Chinese Medicine Hospital), No.1 Fuhua Road, Shenzhen 518033, Guangdong, China, Phone: +86 13530967138, e-mail: qinxiude@foxmail.com

Financial support: This study received funding from the National Natural Science Foundation of China (No. 82405265), Guangdong Basic and Applied Basic Research Foundation (No. 2023A1515110832), Shenzhen Science and Technology Program (Award Numbers: JCYJ20230807094801002, JCYJ20230807094817035)

Conflict of interest: None declared

Background: Ischemic stroke causes severe neurological damage, and promoting angiogenesis in the ischemic penumbra is critical for neurovascular reconstruction and functional recovery. Astragaloside IV (AS-IV) and Tetramethylpyrazine (TMP) are a classic Chinese medicine combination for treating ischemic stroke, yet their synergistic mechanisms are unclear. This study aimed to investigate the enhanced effects of AS-IV combined with TMP on cerebral microvascular endothelial cells following ischemia-reperfusion injury and to explore the regulatory role of the lncRNA MALAT1–CXCL12/CXCR4 signaling axis.

Material/Methods: An oxygen-glucose deprivation/reperfusion (OGD/R) model was established using the bEnd.3 mouse brain microvascular endothelial cell line. Cells were treated with AS-IV, TMP, or their combination to evaluate therapeutic efficacy. Cell viability and migration capacity were assessed using CCK-8, wound healing, and Transwell assays. The expression levels of MALAT1 and angiogenesis-related markers (VEGFA, Ang1, Ang2, CXCL12, and CXCR4) were analyzed via qPCR, western blot, and immunofluorescence. To verify the mechanism, a stable MALAT1 knockdown model was constructed using lentiviral-mediated shRNA transduction.

Results: OGD/R insult significantly reduced cell viability and migration, downregulated MALAT1 expression, and disrupted the Ang1/Ang2 balance. While AS-IV or TMP monotherapy partially mitigated these injuries, the combined treatment demonstrated a greater protective effect than either monotherapy. This enhancement was characterized by upregulation of MALAT1, activation of the CXCL12/CXCR4 pathway, and restoration of VEGFA and Ang1 protein expression. Furthermore, lentiviral-mediated MALAT1 silencing (shMALAT1) markedly impaired cell migration and angiogenic marker expression, effects that were partially rescued by the combined AS-IV and TMP intervention.

Conclusions: The combination of AS-IV and TMP exhibits an enhanced effect compared to either monotherapy in promoting endothelial migration and marker expression in vitro. These findings suggest that the protective mechanism is consistent with the involvement of the MALAT1–CXCL12/CXCR4 signaling axis. This study provides a preliminary cellular rationale for further in vivo validation of this combination therapy in rodent stroke models.

Keywords: Angiogenesis • Cerebral Infarction • Stroke • Neurology • Stroke, Ischemic • Angiogenesis • Long Noncoding RNA MALAT1 • CXCL12 Chemokine • Oxygen-Glucose Deprivation

Full-text PDF: https://www.medscimonit.com/abstract/index/idArt/953474

5852 1 5 38

Publisher's note: All claims expressed in this article are solely those of the authors and do not necessarily represent those of their affiliated organizations, or those of the publisher, the editors and the reviewers. Any product that may be evaluated in this article, or claim that may be made by its manufacturer, is not guaranteed or endorsed by the publisher

APPROVED GALLEY PROOF

This work is licensed under Creative Commons Attribution-NonCommercial-NoDerivatives 4.0 International (CC BY-NC-ND 4.0)

Indexed in: [Current Contents/Clinical Medicine] [SCI Expanded] [ISI Alerting System] [ISI Journals Master List] [Index Medicus/MEDLINE] [EMBASE/Excerpta Medica] [Chemical Abstracts/CAS]

APPROVED GALLEY PROOF

Introduction

Cerebral infarction is the most common type of ischemic stroke and is characterized by a complex pathogenesis, high disability rate, and high recurrence rate, posing a serious threat to global health. According to the latest Global Burden of Disease (GBD) 2021 estimates, stroke causes over 7 million deaths annually, with ischemic strokes accounting for approximately 65% of cases [1]. The global economic burden of stroke is estimated to exceed USD 890 billion annually, accounting for 0.66% of global GDP—a figure projected to nearly double by 2050 [2]. Despite advances in thrombolysis and vascular recanalization, clinical outcomes remain limited by narrow therapeutic windows and reperfusion injury [3]. Consequently, promoting ischemic brain tissue repair and enhancing functional recovery through neurovascular reconstruction have become critical research priorities.

In recent years, increasing evidence has highlighted the essential role of angiogenesis in post-stroke repair. By promoting microvessel regeneration in the ischemic penumbra, angiogenesis improves local perfusion and provides a structural foundation for neuroregeneration. During the reconstruction of the neurovascular unit (NVU), coordinated interactions among neurons, astrocytes, and endothelial cells are crucial for restoring brain function [4-6]. In addition, the formation of collateral circulation complements angiogenesis by enhancing cerebral reperfusion, together forming the core of vascular remodeling following stroke [7-9].

Long non-coding RNA MALAT1 plays a pivotal regulatory role in these processes. Highly expressed in brain microvascular endothelial cells, MALAT1 influences cell proliferation and migration through various epigenetic mechanisms [10]. Specifically, the CXCL12/CXCR4 signaling axis—a key chemotactic pathway independent of the classical VEGF pathway—is critical for the recruitment of endothelial cells and vascular integrity [11,12]. Emerging evidence suggests that MALAT1 can enhance cerebral microvascular angiogenesis by regulating this axis [13]. Thus, the MALAT1–CXCL12/CXCR4 pathway is a promising target for promoting vascular repair.

In traditional Chinese medicine (TCM), astragaloside IV (AS-IV) and tetramethylpyrazine (TMP) constitute a classical "Qi-invigorating and blood-activating" combination [14,15]. Astragaloside IV (AS-IV), one of the major active constituents of astragalus, has been reported to exert multiple pharmacological activities, including immunomodulation, antioxidation, anti-inflammation, protection of the blood–brain barrier (BBB), vascular repair, and neuroprotection [16-18]. Recent studies have further suggested that AS-IV can inhibit apoptosis and regulate lncRNA expression, suggesting its involvement in cerebrovascular repair via epigenetic mechanisms [19].

Tetramethylpyrazine (also known as Ligustrazine, TMP), a major bioactive compound derived from the plant *Ligusticum chuanxiong*, is recognized for its vasodilatory, antiplatelet aggregation, and microcirculation-enhancing properties. TMP has been widely used in TCM-based therapies for ischemic cerebrovascular diseases, including cerebral infarction [20-22].

However, whether their combined application provides enhanced benefits via the MALAT1–CXCL12/CXCR4 signaling pathway remains largely unexplored.

Given their complementary pharmacological profiles, we hypothesize that the combination of AS-IV and TMP can exert a greater protective effect than either monotherapy by co-regulating MALAT1 expression and activating the downstream CXCL12/CXCR4 axis. To test this, we utilized an in vitro oxygen-glucose deprivation/reperfusion (OGD/R) model in bEnd.3 mouse brain microvascular endothelial cells. Through lentiviral-mediated shRNA knockdown of MALAT1, we aimed to investigate whether the vascular protective effects of this combination are mediated through this signaling axis. By elucidating these mechanisms, this study aims to provide a preliminary cellular rationale for the application of TCM-based combination therapies in post-stroke vascular regeneration.

Material and Methods

Reagents and Instruments

Drugs and Reagents

Astragaloside IV (MedChemExpress, Cat. No: HY-N0431); Tetramethylpyrazine (MedChemExpress, Cat. No: HY-N0264); Cell Counting Kit-8 (APExBIO, Cat. No: K1018); RIPA Lysis Buffer (Beyotime, Cat. No: P0013K); Protease Inhibitor Cocktail (Beyotime, Cat. No: P1005); Phosphatase Inhibitor Cocktail (Beyotime, Cat. No: P1081); PMSF (Phenylmethylsulfonyl fluoride, Beyotime, Cat. No: ST507); Enhanced Chemiluminescence (ECL) Substrate (Abbkine, Cat. No: BMU102-CN); 0.5% Trypsin-EDTA (Gibco, Cat. No: 25200-056); DMEM Basic Medium (Gibco, Cat. No: 6125132); PBS (Phosphate-Buffered Saline, BioSharp, Cat. No: BL302A); BCA Protein Assay Kit (Beyotime, Cat. No: P0012); Precast Gel (GenScript, Cat. No: M00657); PVDF Membrane (Merck, Cat. No: ISEQ00010); and Non-fat Milk Powder (Beyotime, Cat No: P0216).

Antibodies

Angiopoietin 1 Polyclonal Antibody (Proteintech, Rabbit-derived, Cat. No: 27093-1-AP, RRID: AB_3085925, Dilution: 1: 1000); Angiopoietin 2 Polyclonal Antibody (Proteintech, Rabbit-derived, Cat. No: 24613-1-AP, RRID: AB_2879639, Dilution: 1: 1000);

This work is licensed under Creative Commons Attribution-NonCommercial-NoDerivatives 4.0 International (CC BY-NC-ND 4.0)

Indexed in: [Current Contents/Clinical Medicine] [SCI Expanded] [ISI Alerting System] [ISI Journals Master List] [Index Medicus/MEDLINE] [EMBASE/Excerpta Medica] [Chemical Abstracts/CAS]

CXCL12/SDF-1 Polyclonal Antibody (Proteintech, Rabbit-derived, Cat. No: 17402-1-AP, RRID: AB_2878404, Dilution: 1: 500); CXCR4 Polyclonal Antibody (Proteintech, Rabbit-derived, Cat. No: 11073-2-AP, RRID: AB_2091813, Dilution: 1: 1000); VEGFA Polyclonal Antibody (Proteintech, Rabbit-derived, Cat. No: 19003-1-AP, RRID: AB_2212657, Dilution: 1: 5000); and β-actin Monoclonal Antibody (Proteintech, Mouse-derived, Cat. No: 66009-1-Ig, RRID: AB_2687938, Dilution: 1: 60000).

Instruments

Mini-PROTEAN® Tetra Electrophoresis System (Bio-Rad, Serial No: 041BR321249); Transwell Inserts (Corning, Cat. No: 353097); Hypoxic Incubator (Billups-Rothenberg, Model: MIC-101); Microplate Reader (BioTek, Model: Synergy H1M); Chemiluminescence Imaging System (Bio-Rad, Model: ChemiDoc); Fluorescence Microscope (ZEISS, Model: Axio Imager M2).

Cell Line

bEnd.3 Cell Line (SUNNCELL, Mouse, Catalogue No: SNL-158, RRID: CVCL_0170).

Cell Culture

The bEnd.3 cell line (mouse brain microvascular endothelial cells) is a stable endothelial cell line derived from brain tissue of mice with hemangioendothelioma. These cells were transformed using the TKmT retroviral vector encoding the middle T antigen of polyomavirus. The endothelial identity of bEnd.3 cells was confirmed by the expression of von Willebrand factor and uptake of fluorescently labeled acetylated low-density lipoprotein.

Cells were cultured under standard conditions in high-glucose Dulbecco's modified Eagle medium (DMEM; Gibco), supplemented with 10% fetal bovine serum (FBS) and 1% penicillin-streptomycin (P/S). Cultures were maintained in a humidified incubator at 37 °C with 5% CO_2. The culture medium was replaced every 2 to 3 days.

Establishment of OGD/R Model

bEnd.3 cells were seeded into 96-well plates at a density of 5000 cells per well and cultured for 24 hours. For the OGD/R experiment, the culture medium was replaced with glucose-free DMEM. The plates were then transferred to a hypoxia chamber and flushed with a gas mixture of 95% N_2 and 5% CO_2 at a low flow rate of 20 L/min for 10 minutes. Subsequently, the chamber inlet and outlet were sealed, and the cells were maintained at 37 °C for 8 hours to induce oxygen-glucose deprivation.

After deprivation, the glucose-free medium was discarded and replaced with complete culture medium. The cells were incubated under normoxic conditions (37 °C, 95% air, 5% CO_2) for 24 hours to allow reoxygenation and glucose restoration. Following this, 10 µL of CCK-8 solution was added to each well, and cells were further incubated for 1.5 hours. Cell viability was then assessed by measuring the absorbance at 450 nm using a microplate reader, and the survival rate was calculated accordingly.

Establishment of MALAT1 Knockdown Model

To establish the MALAT1 knockdown model in bEnd.3 cells, a lentiviral vector system (General Bio [Anhui] Co., Ltd., virus batch number: V1342539, titer: 1.0×10^8 TU/mL) was used. According to the manufacturer's instructions, bEnd.3 cells were seeded into 6-well plates and cultured until reaching 70% to 90% confluency on the day of transduction. Lentiviral suspension was added at a multiplicity of infection (MOI) of 10, along with Polybrene at a final concentration of 8 µg/mL. After thorough mixing, cells were incubated at 37 °C with 5% CO_2 for 24 hours. Following transduction, the medium was replaced with complete culture medium containing 10 µg/mL puromycin for selection, and cells were further cultured for 72 hours. Transduction efficiency was then confirmed by fluorescence microscopy.

Drug Concentration Screening and Grouping

Screening of Safe Concentration Ranges of Drugs

To determine the safe concentration ranges of AS-IV and TMP in bEnd.3 cells, the effects of various drug concentrations on cell viability were assessed using the CCK-8 assay. AS-IV was tested at concentrations of 0, 10, 20, 40, 60, 80, and 100 µM, while TMP concentrations ranged from 0, 10, 50, 100, 150, 200, 250, to 300 µM. Cells were seeded into 96-well plates and allowed to adhere before being treated with different concentrations of the drugs for 24 hours. Subsequently, CCK-8 reagent was added, and the cells were incubated for an additional 1.5 hours. Absorbance (OD) values at 450 nm were measured to evaluate cell viability and determine the safe concentration ranges of the drugs.

Screening of Effective Drug Concentrations in the OGD/R Model

Based on the previously determined safe concentration ranges, effective intervention concentrations of the drugs were further screened in bEnd.3 cells subjected to OGD/R treatment. AS-IV was tested at concentrations of 20, 60, and 100 µM, while TMP was tested at 50, 100, 150, and 300 µM. After

APPROVED GALLEY PROOF

This work is licensed under Creative Commons Attribution-NonCommercial-NoDerivatives 4.0 International (CC BY-NC-ND 4.0)

Indexed in: [Current Contents/Clinical Medicine] [SCI Expanded] [ISI Alerting System] [ISI Journals Master List] [Index Medicus/MEDLINE] [EMBASE/Excerpta Medica] [Chemical Abstracts/CAS]

APPROVED GALLEY PROOF

treating the model cells for 24 hours, cell viability was assessed using the CCK-8 assay to identify the most appropriate intervention doses.

Experimental Grouping

Based on the preliminary screening results, AS-IV at 100 μM and TMP at 300 μM were selected as the intervention concentrations for subsequent experiments. The cell experiments were divided into the following 5 groups:
Control group: bEnd.3 cells cultured under normal conditions;
OGD/R group: OGD/R model established on the Control group;
AS-IV group: OGD/R model treated with AS-IV (100 μM);
TMP group: OGD/R model treated with TMP (300 μM);
AS-IV + TMP group: OGD/R model treated with a combination of AS-IV (100 μM) and TMP (300 μM).

Construction of MALAT1 Knockdown Model and Experimental Grouping

To further investigate the role of MALAT1 in the protective effects of the AS-IV and TMP combination, a stable MALAT1 knockdown model was established using lentiviral-mediated shRNA transduction. The experimental groups were defined as follows:
shCon group: bEnd.3 cells transduced with a scrambled control shRNA lentiviral vector, serving as the negative control.
shMALAT1 group: bEnd.3 cells transduced with a MALAT1-targeting shRNA lentiviral vector to silence MALAT1 expression.
shMALAT1 + AS-IV group: shMALAT1 cells treated with AS-IV (100 μM).
shMALAT1 + TMP group: shMALAT1 cells treated with TMP (300 μM).
shMALAT1 + AS-IV + TMP group: shMALAT1 cells treated with a combination of AS-IV (100 μM) and TMP (300 μM).

Cell Viability Assay

bEnd.3 cells in the logarithmic growth phase were seeded into 96-well plates at a density of 5000 cells per well. According to the experimental grouping, the respective models were established, and culture media containing varying concentrations of the test drugs were added. After 24 hours of incubation, 10 μL of CCK-8 solution was added to each well, followed by incubation in the dark for 1.5 hours. The absorbance (OD) was measured at 450 nm using a microplate reader, and cell viability was calculated accordingly.

Cell Scratch Assay

bEnd.3 cells were seeded into 6-well plates at a density of 200 000 cells per well and cultured until reaching over 90% confluence. A sterile 200 μL pipette tip was used to create a straight scratch vertically across the center of each well, producing a uniform wound area. The wells were gently washed twice with PBS to remove detached cells and debris. The medium was then replaced with culture medium containing 1% FBS, and the appropriate treatments were applied according to the experimental groups. Cells were incubated at 37 °C in a 5% CO_2 atmosphere. Images of the scratched areas were captured at 0 and 24 hours using an inverted microscope. Scratch widths were measured using ImageJ software, and cell migration rate was calculated using the following formula: Cell migration rate (%) = [(Initial scratch area - Scratch area at 24 h) / Initial scratch area] × 100%.

Transwell Cell Migration Assay

bEnd.3 cells from each treatment group were resuspended in serum-free medium and seeded into the upper chambers of 24-well Transwell inserts at a density of 50 000 cells per well. The lower chambers were filled with 600 μL of complete medium containing 10% FBS as a chemoattractant. Cells were incubated at 37 °C in a humidified atmosphere with 5% CO_2 for 24 hours. After incubation, Transwell inserts were carefully removed and washed twice with PBS. Non-migrated cells on the upper surface of the membrane were gently wiped off with a cotton swab. Cells that migrated to the lower surface were fixed with 4% paraformaldehyde for 15 minutes and stained with 0.1% crystal violet for 20 minutes. Following thorough washing with PBS, the membranes were air-dried. Five random fields per insert were photographed under an inverted microscope, and the average number of migrated cells was calculated.

Quantitative PCR (qPCR)

Total RNA was extracted from cells using TRIzol reagent. RNA concentration and purity were measured using a NanoDrop spectrophotometer. One microgram of RNA was reverse-transcribed into cDNA using the PrimeScript™ RT reagent kit. qPCR reactions were performed on a QuantStudio 5 system using TB Green Premix (Takara). Each 20 μL reaction mixture contained 10 μL of TB Green Premix, 0.4 μL of each primer (10 μM), 2 μL of cDNA, and nuclease-free water. The thermal cycling program consisted of an initial denaturation at 95 °C for 30 seconds, followed by 40 cycles of 95 °C for 5 seconds and 60 °C for 30 seconds. Melt curve analysis was conducted to verify amplification specificity. Primers for the target genes and sequences were synthesized by Sangon Biotech Co., Ltd. (Shanghai, China), with β-actin used as the internal control. All samples were run in triplicate, and relative gene expression levels were calculated using the $2^{-\Delta\Delta Ct}$ method.

Western Blot Analysis

Treated cells were collected and lysed on ice for 20 minutes using lysis buffer. The lysates were sonicated 3 times for 15

This work is licensed under Creative Commons Attribution-NonCommercial-NoDerivatives 4.0 International (CC BY-NC-ND 4.0)

Indexed in: [Current Contents/Clinical Medicine] [SCI Expanded] [ISI Alerting System] [ISI Journals Master List] [Index Medicus/MEDLINE] [EMBASE/Excerpta Medica] [Chemical Abstracts/CAS]

seconds each at 4 °C, followed by centrifugation at 12 000 rpm for 20 minutes at 4 °C. The supernatant containing total cellular protein was collected. Protein concentration was determined using a BCA assay kit. Protein samples were mixed with loading buffer and denatured by heating at 100 °C for 10 minutes. Proteins were separated by 4% to 20% SDS-PAGE and transferred onto PVDF membranes. Membranes were blocked at room temperature for 60 minutes with 5% non-fat milk or rapid western blot blocking solution. Membranes were incubated overnight at 4 °C with primary antibodies against CXCR4, Ang1, Ang2, and VEGFA. After 3 washes with TBST, membranes were incubated with secondary antibodies at room temperature for 60 minutes. Following 3 additional TBST washes, protein bands were visualized using enhanced chemiluminescence (ECL) reagents. Band intensities were quantified using Image Lab software, and relative protein expression levels were normalized to β-actin.

Immunofluorescence (IF) Staining

bEnd.3 cells were seeded at 50 000 cells per well onto coverslips placed in 12-well plates. After reaching an appropriate confluence, experimental models were established, and culture media containing various concentrations of drugs were added according to the grouping. Upon completion of treatment, cells were gently washed 3 times with PBS and fixed with 4% paraformaldehyde for 15 minutes. After fixation, cells were washed 3 times with PBS for 5 minutes each. Cells were then permeabilized with 0.3% Triton X-100 (dissolved in PBS) at room temperature for 20 minutes, followed by 3 additional PBS washes. To block nonspecific binding, cells were incubated with 5% BSA at room temperature for 60 minutes. Primary antibodies against CXCL12, CXCR4, Ang1, and Ang2 were applied, and samples were incubated overnight at 4 °C. The following day, cells were washed 3 times with PBS (5 minutes each) and incubated with fluorescently labeled secondary antibodies for 1 hour in the dark. After staining, cells were washed 3 times with PBS. Nuclear staining was performed using DAPI and incubated for 5 minutes at room temperature in the dark, followed by a final PBS wash. Coverslips were mounted onto glass slides and observed under a fluorescence microscope for imaging.

Statistical Analysis

Statistical analyses were conducted using SPSS version 19.0. Data are presented as mean ± SD from 3 independent biological replicates. Post hoc comparisons were performed using Tukey's HSD test following one-way ANOVA. If these assumptions were violated, Welch's ANOVA was applied, followed by Games–Howell post hoc tests for multiple comparisons. A P value less than 0.05 was considered statistically significant.

Results

Screening of OGD/R Model Duration and Drug Concentrations

Optimal OGD/R Treatment Duration for bEnd.3 Cells

CCK-8 assay results showed that cell viability gradually decreased with prolonged OGD exposure (**Figure 1A**). Considering the extent of cellular injury and the practicality of the model, 8 hours of OGD treatment resulted in approximately 85% cell viability, effectively simulating a moderate ischemic state. This duration induced significant ischemic injury responses while maintaining sufficient cell viability for subsequent functional studies, such as angiogenesis. Therefore, we selected 8 hours of OGD followed by 24 hours of reoxygenation and glucose reperfusion as the optimal treatment duration for establishing the bEnd.3 OGD/R model.

Safety Concentration Ranges of Astragaloside IV and Tetramethylpyrazine in bEnd.3 Cells

CCK-8 assay results demonstrated that astragaloside IV (AS-IV) exhibited no significant cytotoxicity toward bEnd.3 cells within the concentration range of 0 to 100 μM, with cell viability at all concentrations remaining comparable to the control group (**Figure 1B**). Similarly, Tetramethylpyrazine (TMP) showed no notable cytotoxic effects within the 0 to 300 μM concentration range (**Figure 1C**), indicating good biocompatibility of both compounds at the tested concentrations.

Effective Concentration Screening of Drugs in the OGD/R Model

Within the OGD/R model, AS-IV significantly enhanced cell viability in a concentration-dependent manner, with the most pronounced protective effect observed at 100 μM (**Figure 1D**). TMP also demonstrated a dose-dependent cytoprotective effect, showing the greatest efficacy at 300 μM (**Figure 1E**). Consequently, AS-IV at 100 μM and TMP at 300 μM were selected as the intervention concentrations for subsequent experiments.

OGD/R Model Results

Protective Effects of Drugs on Cell Injury in the OGD/R Model

The effects of AS-IV and TMP on cell viability in the bEnd.3 OGD/R model were evaluated using the CCK-8 assay. Compared with the Control group, cell viability in the OGD/R group significantly decreased ($P < 0.001$), confirming the successful establishment of the ischemia-reperfusion injury model. Treatment with AS-IV (100 μM) or TMP (300 μM) following OGD/R significantly

APPROVED GALLEY PROOF

This work is licensed under Creative Commons Attribution-NonCommercial-NoDerivatives 4.0 International (CC BY-NC-ND 4.0)

Indexed in: [Current Contents/Clinical Medicine] [SCI Expanded] [ISI Alerting System] [ISI Journals Master List] [Index Medicus/MEDLINE] [EMBASE/Excerpta Medica] [Chemical Abstracts/CAS]

APPROVED GALLEY PROOF

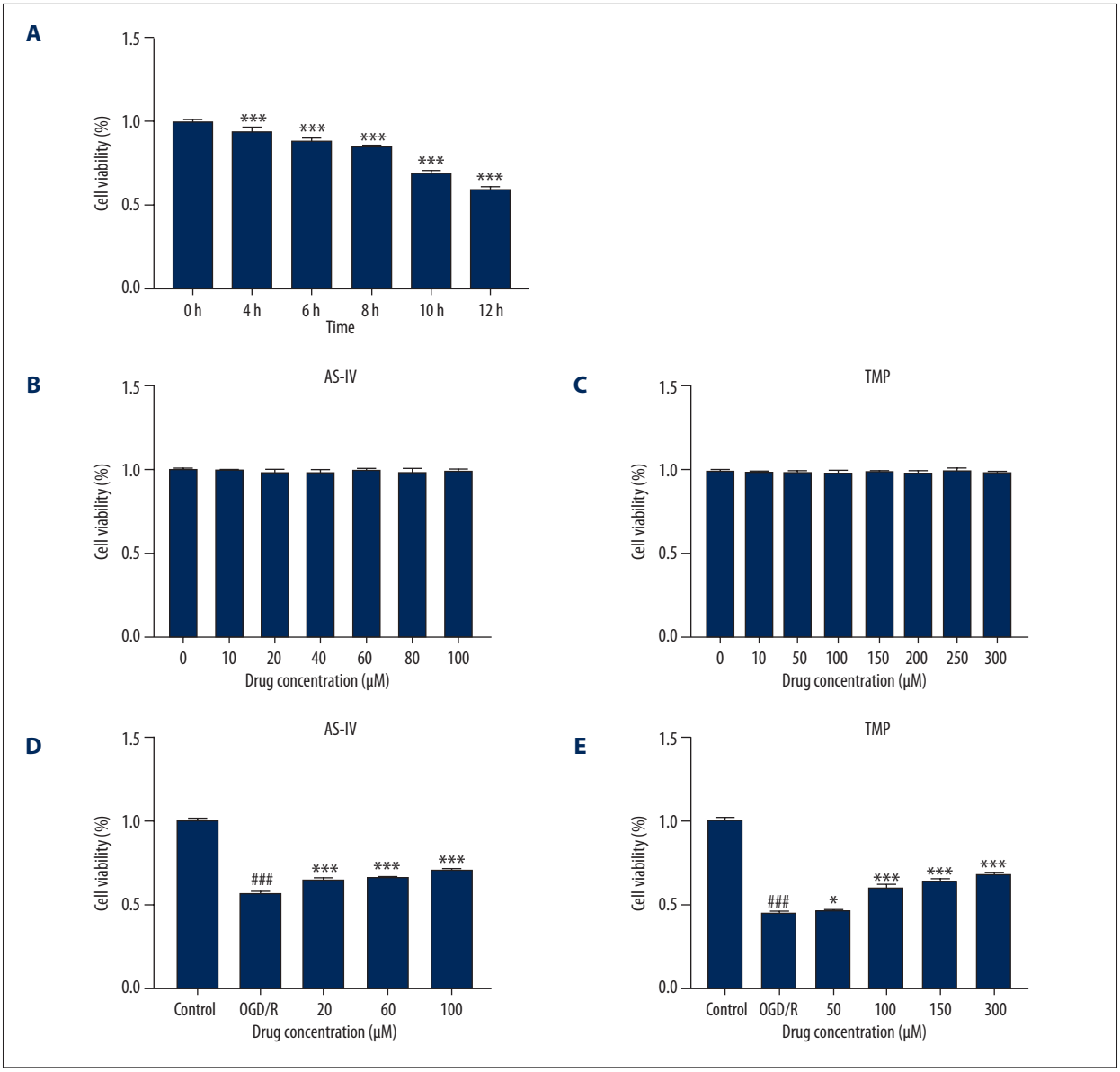

Figure 1. Determination of optimal OGD/R modeling conditions and drug concentrations in bEnd.3 cells. (**A**) Cell viability of bEnd.3 cells subjected to different durations of oxygen-glucose deprivation (OGD), assessed via CCK-8 assay. Cell viability progressively declined with increasing OGD exposure durations compared to the Control group ($P < 0.001$). An 8-hour OGD treatment followed by 24-hour reoxygenation resulted in approximately 85% viability, representing a stable and reproducible ischemic injury model suitable for downstream experiments. (**B**) Effect of various concentrations of AS-IV (0-100 μM) on bEnd.3 cell viability. No significant cytotoxicity was observed across the tested range under physiological conditions. (**C**) Effect of various concentrations of TMP (0-300 μM) on bEnd.3 cell viability. Cell viability remained comparable to the Control group, indicating favorable biocompatibility of TMP within this concentration range. (**D**) Evaluation of AS-IV at different concentrations (20, 60, 100 μM) in the OGD/R model. AS-IV at 100 μM produced the most significant increase in cell viability compared to the OGD/R group ($P < 0.001$). (**E**) Evaluation of TMP at different concentrations (50, 100, 150, 300 μM) in the OGD/R model. TMP at 300 μM showed the most potent protective effect compared to the OGD/R group ($P < 0.001$). Data are presented as mean ± SD from 3 independent experiments. ### $P < 0.001$ vs Control group; * $P < 0.05$, *** $P < 0.001$ vs OGD/R group, as indicated.

This work is licensed under Creative Commons Attribution-NonCommercial-NoDerivatives 4.0 International (CC BY-NC-ND 4.0)

Indexed in: [Current Contents/Clinical Medicine] [SCI Expanded] [ISI Alerting System] [ISI Journals Master List] [Index Medicus/MEDLINE] [EMBASE/Excerpta Medica] [Chemical Abstracts/CAS]

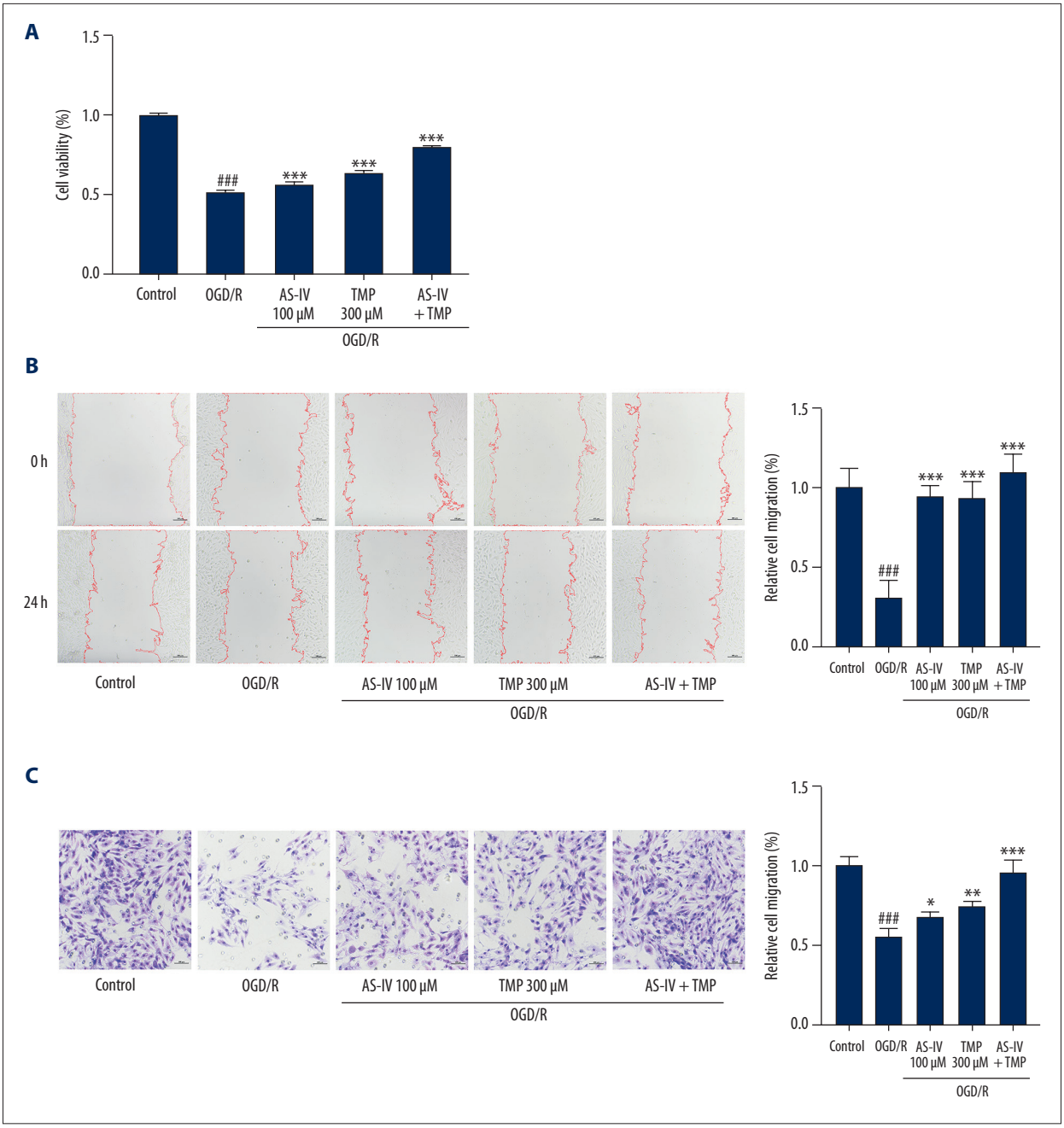

Figure 2. AS-IV and TMP promote bEnd.3 cell viability and migration under OGD/R conditions. (**A**) Cell viability assessed by CCK-8 assay. OGD/R significantly reduced cell viability compared to the Control group ($P < 0.001$). Treatment with AS-IV (100 μM) or TMP (300 μM) significantly improved cell viability compared to the OGD/R group ($P < 0.001$), and the combined treatment (AS-IV + TMP) exhibited a significantly more pronounced protective effect compared to either monotherapy ($P < 0.001$). (**B**) Wound healing assay to evaluate the migration capacity of bEnd.3 cells. Cell migration was significantly reduced in the OGD/R group compared to the Control group ($P < 0.001$). Treatment with AS-IV (100 μM) or TMP (300 μM) significantly accelerated wound closure ($P < 0.001$), with the combined treatment showing the most significant enhancement ($P < 0.001$). (**C**) Transwell migration assay. OGD/R insult markedly reduced the number of migrated cells ($P < 0.001$). Both AS-IV and TMP treatments significantly enhanced cell migration ($P < 0.05$), and the combined treatment exhibited an enhanced combined effect ($P < 0.001$). Data are presented as mean ± SD from 3 independent experiments. ### $P < 0.001$ vs Control group; * $P < 0.05$, ** $P < 0.01$, *** $P < 0.001$ vs OGD/R group, as indicated.

APPROVED GALLEY PROOF

This work is licensed under Creative Commons Attribution-NonCommercial-NoDerivatives 4.0 International (CC BY-NC-ND 4.0)

Indexed in: [Current Contents/Clinical Medicine] [SCI Expanded] [ISI Alerting System] [ISI Journals Master List] [Index Medicus/MEDLINE] [EMBASE/Excerpta Medica] [Chemical Abstracts/CAS]

APPROVED GALLEY PROOF

Table 1. Primer sequences used for qPCR analysis of target genes.

Gene	Primer direction	Sequence (5'→3')	Product size (bp)
CXCL12	Forward	GCACGGCTGAAGAACAA	249
CXCL12	Reverse	AAGAGGGAGGAGCGAGT	
CXCR4	Forward	CTGTGACCGCCTTTACC	265
CXCR4	Reverse	TCCTTGCTTGATGACCC	
lncRNA MALAT1	Forward	TGACTCAAGGGAACCAG	151
lncRNA MALAT1	Reverse	AAGAGTAAACTACCAGCAA	
β-actin	Forward	TCGTGCGTGACATCAAAGA	184
β-actin	Reverse	CATACCCAAGAAGGAAGGCT	

The nucleotide sequences of forward and reverse primers used for quantitative real-time PCR (qPCR) analysis of mRNA expression levels of MALAT1, CXCL12, CXCR4, and housekeeping gene β-actin. All primers were synthesized by Sangon Biotech (Shanghai) Co., Ltd., China.

improved cell viability ($P < 0.001$). Notably, the combined treatment with AS-IV and TMP resulted in a significantly greater increase in cell viability compared to either monotherapy ($P < 0.001$), suggesting an enhanced protective effect under these experimental conditions (**Figure 2A**).

Effects of AS-IV and TMP on Migration Ability of bEnd.3 Cells

In the wound healing assay, the migration capacity of cells in the OGD/R group was significantly reduced compared to the Control group ($P < 0.001$), indicating that ischemia-reperfusion injury markedly impaired endothelial cell migration. Treatment with AS-IV (100 μM) or TMP (300 μM) significantly accelerated wound closure compared to the OGD/R group ($P < 0.001$). Notably, the combined treatment further enhanced the cell migration rate to a level significantly higher than that of either monotherapy ($P < 0.001$). In the Transwell migration assay, the number of cells migrating through the membrane was significantly decreased following OGD/R treatment ($P < 0.001$). Both AS-IV and TMP alone significantly promoted cell migration ($P < 0.05$). The combined intervention showed the most pronounced effect ($P < 0.001$), demonstrating an enhanced pro-migratory effect compared to single-drug treatments (**Figure 2B, 2C**).

Changes in MALAT1 and Related Gene Expression in the OGD/R Model

To investigate whether the protective effects of AS-IV and TMP on OGD/R-treated bEnd.3 cells are mediated through MALAT1, qPCR was performed to assess MALAT1 expression levels. The primers and target genes were synthesized by Sangon Biotech (Shanghai) Co., Ltd., China (detailed in **Table 1**). Results showed that MALAT1 expression was significantly decreased in the OGD/R group compared to the Control group ($P < 0.01$). Treatment with AS-IV (100 μM) or TMP (300 μM) after OGD/R significantly upregulated MALAT1 expression compared to the OGD/R group ($P < 0.05$). Notably, the combined treatment (AS-IV + TMP) resulted in a significantly higher upregulation of MALAT1 compared to either monotherapy ($P < 0.05$), demonstrating an enhanced effect of the combination in modulating MALAT1 gene expression (**Figure 3A**).

Expression of Angiogenesis-Related Proteins in the OGD/R Model

Western blot analysis showed that the expression levels of CXCR4 and VEGFA were significantly increased in the OGD/R group compared to the Control group ($P < 0.01$). Treatment with AS-IV (100 μM) or TMP (300 μM) alone further increased the expression of these 2 proteins, although the differences were not statistically significant. In contrast, the combined treatment (AS-IV + TMP) resulted in a significantly more pronounced upregulation of CXCR4 and VEGFA ($P < 0.01$) compared to either monotherapy, demonstrating an enhanced combined effect.

Regarding vascular stability markers, Ang1 expression was significantly downregulated in the OGD/R group ($P < 0.01$), while Ang2 was upregulated ($P < 0.05$), leading to a marked increase in the Ang2/Ang1 ratio ($P < 0.01$). Treatment with either AS-IV or TMP reversed these changes by increasing Ang1 and decreasing Ang2 expression, thereby significantly reducing the Ang2/Ang1 ratio. Notably, the combined treatment showed the most prominent effect in restoring the Ang2/Ang1 balance. These results are consistent with the hypothesis that AS-IV and TMP can promote vascular stability and potentially reduce vascular leakage by restoring the balance between Ang2 and Ang1 in this in vitro model (**Figure 3B**).

This work is licensed under Creative Commons Attribution-NonCommercial-NoDerivatives 4.0 International (CC BY-NC-ND 4.0)

Indexed in: [Current Contents/Clinical Medicine] [SCI Expanded] [ISI Alerting System] [ISI Journals Master List] [Index Medicus/MEDLINE] [EMBASE/Excerpta Medica] [Chemical Abstracts/CAS]

Immunofluorescence Staining Results

Immunofluorescence analysis revealed that Ang1 expression was significantly decreased in the OGD/R group ($P < 0.001$). Following drug treatment, both AS-IV and TMP monotherapy partially restored Ang1 expression, while the combined treatment (AS-IV + TMP) led to a significantly more pronounced upregulation compared to either monotherapy ($P < 0.001$). In contrast, Ang2 expression was elevated in the OGD/R group; drug interventions reduced Ang2 levels, with the most substantial reduction observed in the combined treatment group ($P < 0.001$).

Regarding the chemotactic signaling axis, OGD/R stimulation led to a slight increase in CXCL12 and CXCR4 expression, although the upregulation of CXCL12 did not reach statistical significance. Monotherapy with AS-IV or TMP showed an upward trend in the expression of these markers without statistical significance compared to the OGD/R group. Notably, combined treatment significantly enhanced the expression of both CXCL12 and CXCR4 ($P < 0.001$). These findings are consistent with the hypothesis that AS-IV and TMP can exert an enhanced combined effect in activating the CXCL12/CXCR4 signaling pathway, which is critical for endothelial migration and vascular repair in this in vitro model (**Figure 3C**).

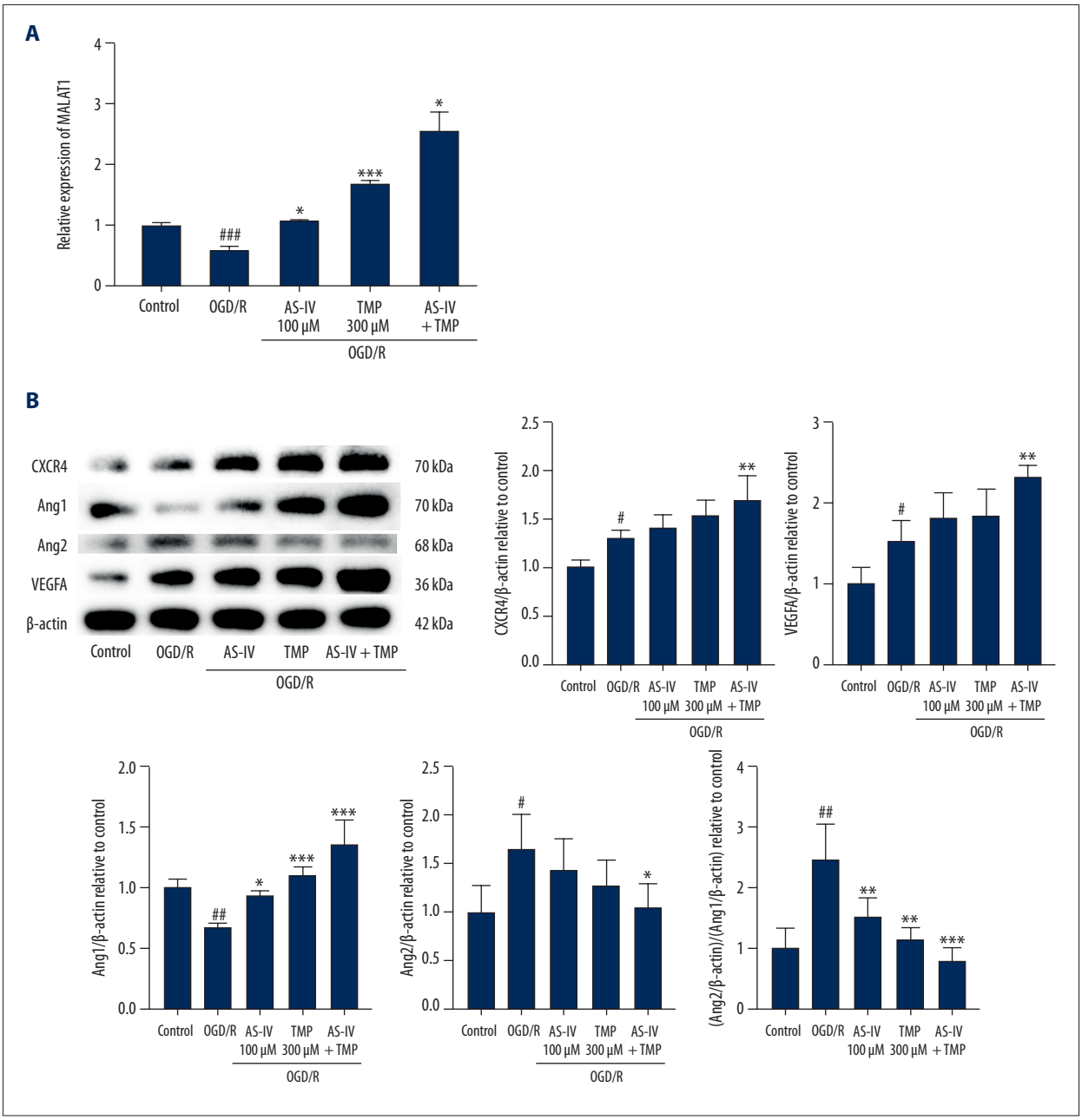

APPROVED GALLEY PROOF

This work is licensed under Creative Commons Attribution-NonCommercial-NoDerivatives 4.0 International (CC BY-NC-ND 4.0)

Indexed in: [Current Contents/Clinical Medicine] [SCI Expanded] [ISI Alerting System] [ISI Journals Master List] [Index Medicus/MEDLINE] [EMBASE/Excerpta Medica] [Chemical Abstracts/CAS]

APPROVED GALLEY PROOF

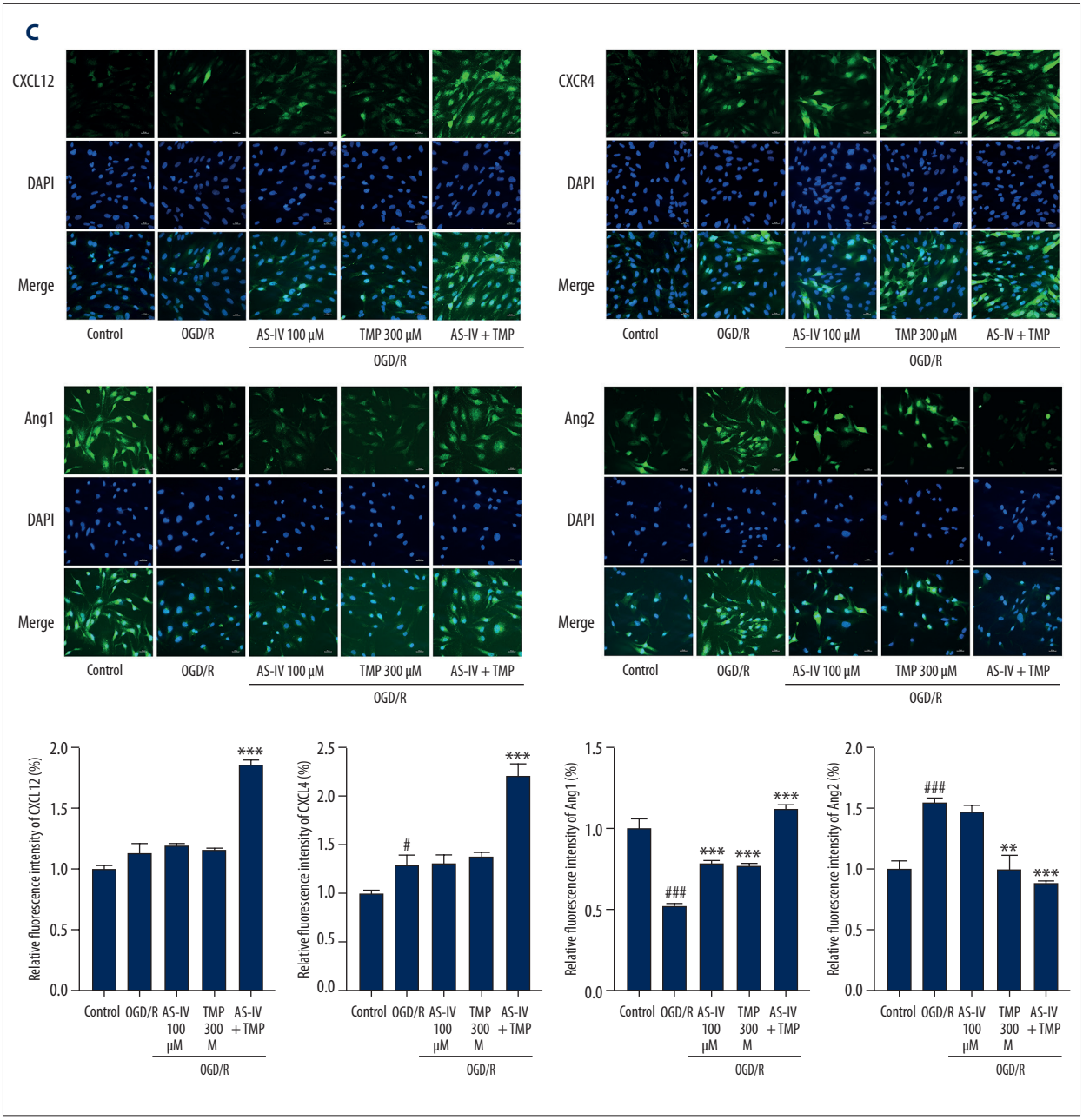

Figure 3. Effects of AS-IV and TMP on MALAT1 expression and angiogenesis-related proteins in bEnd.3 cells under OGD/R conditions. (**A**) qPCR analysis of MALAT1 expression. OGD/R injury significantly suppressed MALAT1 transcription ($P < 0.01$). Monotherapies partially restored its levels ($P < 0.05$), while combined treatment (AS-IV + TMP) led to a significantly more pronounced upregulation compared to either monotherapy. (**B**) Western blot analysis of CXCR4, VEGFA, Ang1, and Ang2. OGD/R significantly upregulated CXCR4 and VEGFA ($p < 0.01$), downregulated Ang1 ($p < 0.01$), and upregulated Ang2 ($P < 0.05$), increasing the Ang2/Ang1 ratio ($P < 0.01$). Combined treatment significantly enhanced CXCR4 and VEGFA expression ($P < 0.01$) and uniquely optimized the Ang1/Ang2 balance compared to the OGD/R group. (**C**) Immunofluorescence staining of Ang1, Ang2, CXCL12, and CXCR4. Combined treatment significantly reversed the OGD/R-induced decrease in Ang1 and increase in Ang2 ($P < 0.001$). Marked elevations in CXCL12 and CXCR4 levels were observed predominantly in the combination group ($P < 0.001$), showing an enhanced combined effect. Data are presented as mean ± SD from 3 independent experiments. $^{\#}P < 0.05$, $^{\#\#}P < 0.01$, $^{\#\#\#}P < 0.001$ vs Control group; $^{*}P < 0.05$, $^{**}P < 0.01$, $^{***}P < 0.001$ vs OGD/R group, as indicated.

This work is licensed under Creative Commons Attribution-NonCommercial-NoDerivatives 4.0 International (CC BY-NC-ND 4.0)

Indexed in: [Current Contents/Clinical Medicine] [SCI Expanded] [ISI Alerting System] [ISI Journals Master List] [Index Medicus/MEDLINE] [EMBASE/Excerpta Medica] [Chemical Abstracts/CAS]

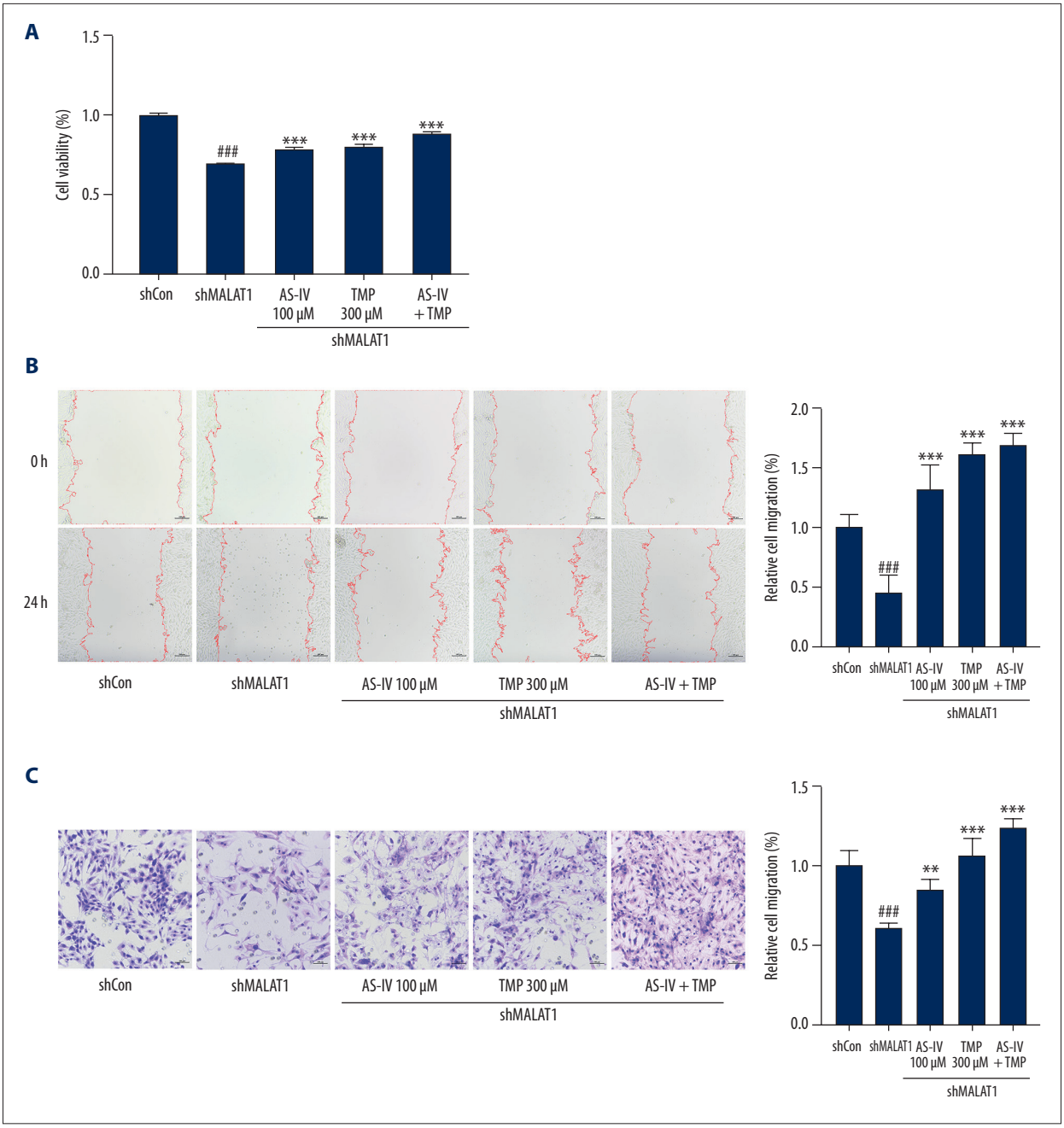

Figure 4. Effects of MALAT1 silencing on cell viability and migration, and the protective role of AS-IV and TMP in bEnd.3 cells. (**A**) CCK-8 assay for cell viability. Cells were transduced with lentiviral shRNA (shMALAT1 or shCon) prior to OGD/R. MALAT1 silencing markedly reduced cell viability ($P < 0.001$). Monotherapies partially rescued this decline, whereas the combined treatment exhibited a significantly greater protective effect ($P < 0.001$). (**B**) Wound healing assay. Knockdown of MALAT1 significantly impaired scratch closure ($P < 0.001$). Combined treatment demonstrated a significantly enhanced recovery in migration capacity compared to monotherapies ($P < 0.001$). (**C**) Transwell migration assay. The shMALAT1 group showed a profound reduction in migrated cell counts ($P < 0.001$), which was most effectively counteracted by the combination of AS-IV and TMP ($P < 0.001$). Data are expressed as mean ± SD from 3 independent experiments. ### $P < 0.001$ vs shCon group; ** $P < 0.01$, *** $P < 0.001$ vs shMALAT1 group, as indicated.

APPROVED GALLEY PROOF

This work is licensed under Creative Commons Attribution-NonCommercial-NoDerivatives 4.0 International (CC BY-NC-ND 4.0)

Indexed in: [Current Contents/Clinical Medicine] [SCI Expanded] [ISI Alerting System] [ISI Journals Master List] [Index Medicus/MEDLINE] [EMBASE/Excerpta Medica] [Chemical Abstracts/CAS]

APPROVED GALLEY PROOF

Validation of MALAT1 Knockdown Model

Effects of MALAT1 Silencing on Cell Viability and Drug Intervention

Following the construction of the MALAT1 knockdown model via lentiviral-mediated shRNA transduction, cell viability in the shMALAT1 group was significantly lower than in the shCon group ($P < 0.001$). This indicates that MALAT1 plays a critical role in maintaining the viability of bEnd.3 cells. Treatment with AS-IV or TMP partially reversed the reduction in viability caused by MALAT1 silencing ($P < 0.001$). Notably, the combined treatment (shMALAT1 + AS-IV + TMP) resulted in a significantly greater enhancement of cell viability compared to either monotherapy ($P < 0.001$), suggesting an enhanced combined effect even under conditions of MALAT1 deficiency (**Figure 4A**).

Effects of MALAT1 Silencing on Cell Migration and Drug Intervention

Compared with the shCon group, the shMALAT1 group exhibited significantly less wound healing and Transwell migration capacity ($P < 0.001$), confirming that MALAT1 plays a critical regulatory role in endothelial cell migration. Under conditions

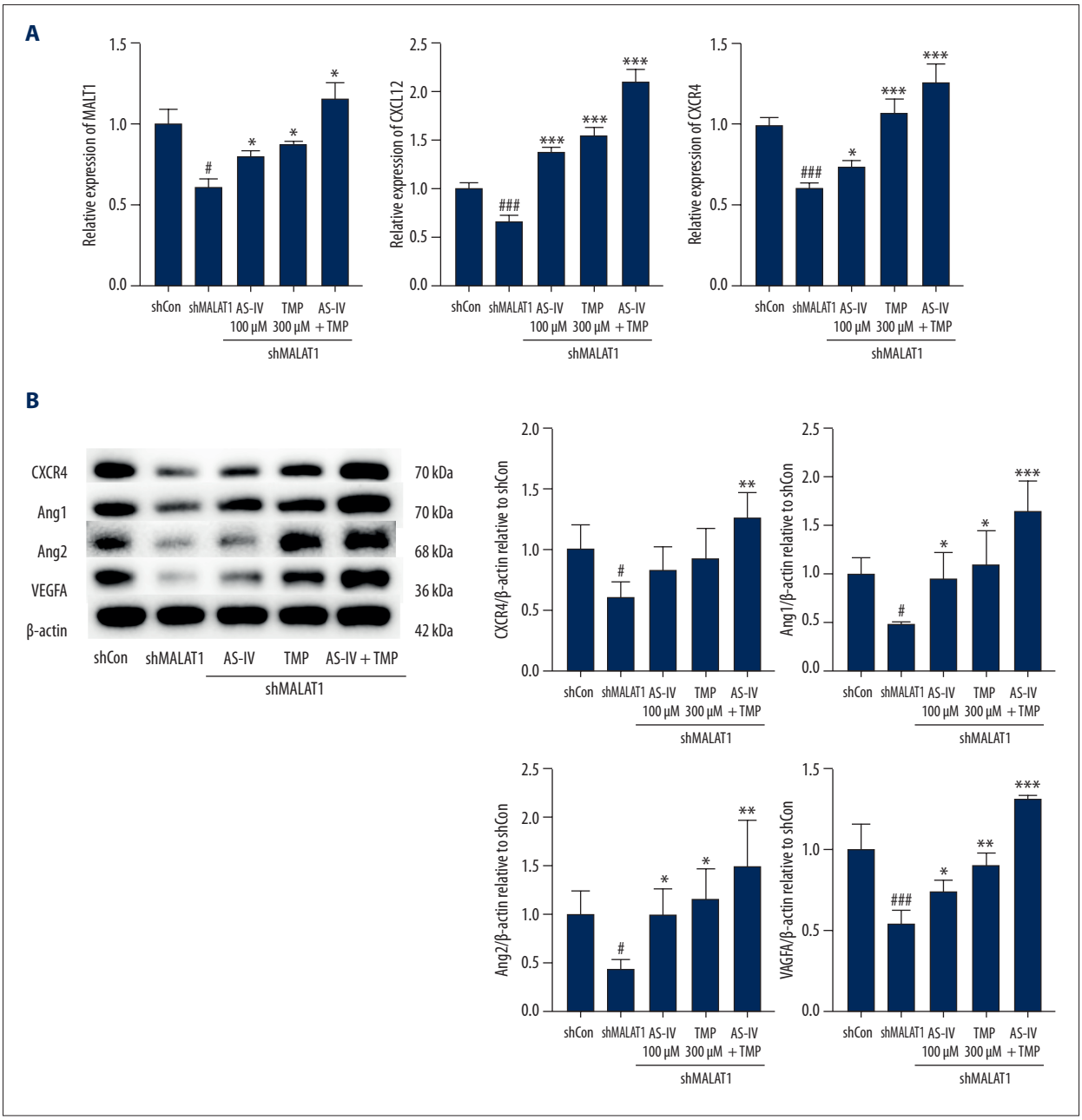

This work is licensed under Creative Commons Attribution-NonCommercial-NoDerivatives 4.0 International (CC BY-NC-ND 4.0)

Indexed in: [Current Contents/Clinical Medicine] [SCI Expanded] [ISI Alerting System] [ISI Journals Master List] [Index Medicus/MEDLINE] [EMBASE/Excerpta Medica] [Chemical Abstracts/CAS]

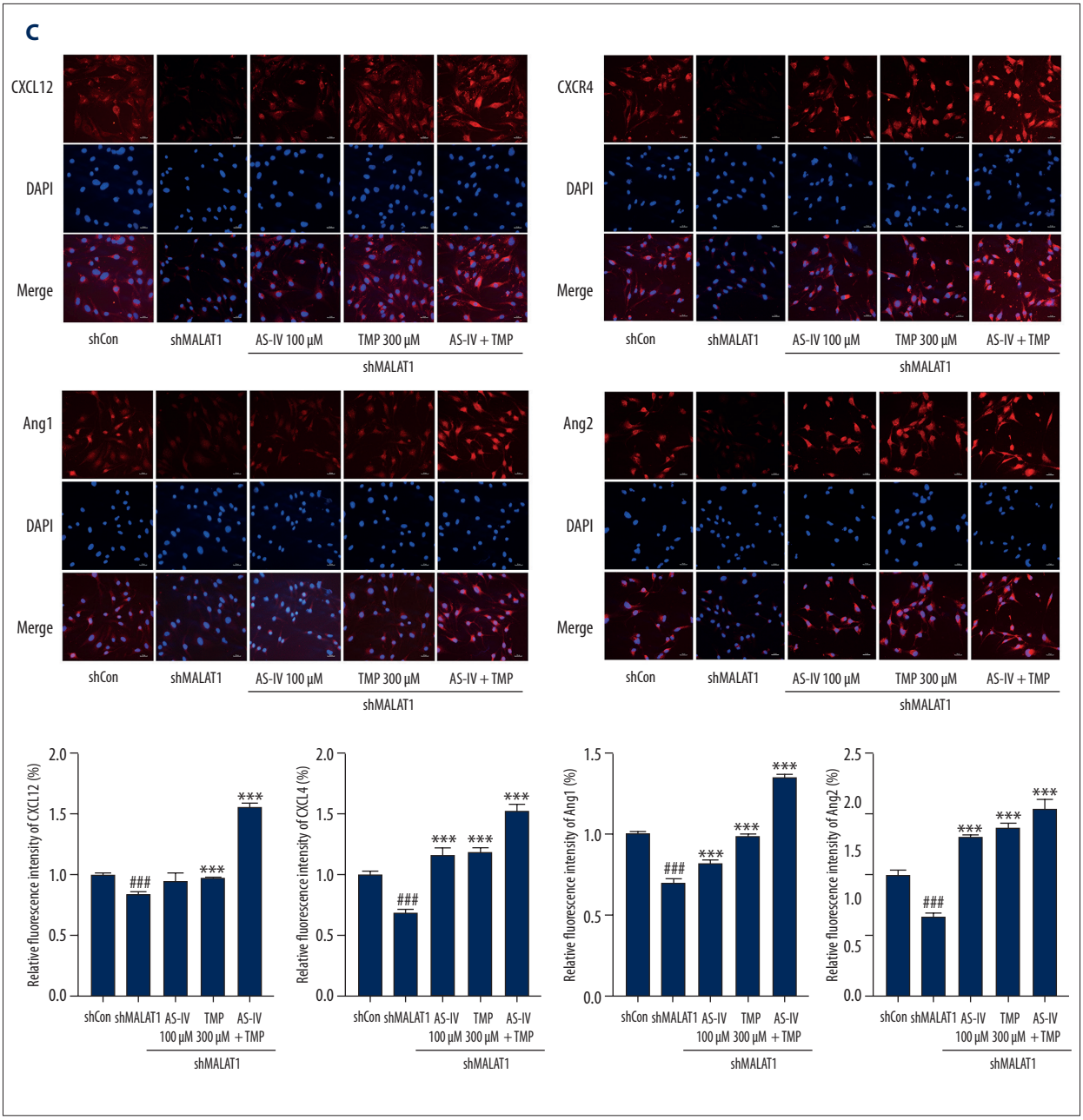

Figure 5. Regulation of the CXCL12/CXCR4 axis and angiogenesis-related proteins by MALAT1 and drug interventions in bEnd.3 cells. (**A**) qPCR analysis of MALAT1, CXCL12, and CXCR4 mRNA. MALAT1 knockdown drastically reduced the transcription of all 3 genes ($P < 0.05$). Combined drug treatment significantly upregulated CXCL12 and CXCR4 expression compared to the shMALAT1 group ($P < 0.001$), indicating positive regulation by MALAT1. (**B**) Western blot analysis of CXCR4, VEGFA, Ang1, and Ang2. Protein levels were significantly suppressed following MALAT1 silencing ($P < 0.05$). Combined treatment produced a significantly more pronounced recovery compared to either monotherapy ($P < 0.01$), showing that the effects are partially mediated via MALAT1. (**C**) Immunofluorescence staining of CXCL12, CXCR4, Ang1, and Ang2. Expression of all 4 proteins collapsed after MALAT1 silencing. Combination therapy significantly restored their levels ($P < 0.001$), supporting MALAT1 as a crucial upstream regulator associated with vascular repair. Data are presented as mean ± SD from 3 independent experiments. $^{\#}P < 0.05$, $^{\#\#}P < 0.01$, $^{\#\#\#}P < 0.001$ vs shCon group; $^{*}P < 0.05$, $^{**}P < 0.01$, $^{***}P < 0.001$ vs shMALAT1 group, as indicated.

APPROVED GALLEY PROOF

This work is licensed under Creative Commons Attribution-NonCommercial-NoDerivatives 4.0 International (CC BY-NC-ND 4.0)

Indexed in: [Current Contents/Clinical Medicine] [SCI Expanded] [ISI Alerting System] [ISI Journals Master List] [Index Medicus/MEDLINE] [EMBASE/Excerpta Medica] [Chemical Abstracts/CAS]

APPROVED GALLEY PROOF

of MALAT1 silencing, treatment with AS-IV or TMP partially restored cell migration ability compared to the shMALAT1 group ($P < 0.01$). Notably, the combined treatment (shMALAT1 + AS-IV + TMP) resulted in a significantly more pronounced improvement compared to either monotherapy ($P < 0.001$). These findings suggest that while the pro-migratory effects of AS-IV and TMP are partially dependent on MALAT1, the combination exerts an enhanced combined effect that can also involve additional pathways (**Figure 4B, 4C**).

Regulation of CXCL12/CXCR4 and Related Gene Expression by MALAT1 Silencing

Following lentiviral-mediated transduction, mRNA expression levels of MALAT1, CXCL12, and CXCR4 in the shMALAT1 group were significantly lower compared to the shCon group ($P < 0.05$). This confirmed that MALAT1 silencing led to a coordinated downregulation of the CXCL12/CXCR4 signaling axis. Treatment with AS-IV or TMP partially reversed the downregulation of these genes. Notably, the combined treatment (shMALAT1 + AS-IV + TMP) resulted in a significantly greater enhancement of CXCL12 and CXCR4 expression compared to either monotherapy ($P < 0.001$). These results are consistent with the hypothesis that the AS-IV and TMP combination exerts its regulatory effects on the CXCL12/CXCR4 axis at least in part through the modulation of MALAT1 (**Figure 5A**).

Effects of MALAT1 Silencing on the Expression of Angiogenesis-Related Proteins

Western blot analysis demonstrated that in the shMALAT1 group, the protein expression levels of CXCR4, VEGFA, Ang1, and Ang2 were significantly lower than in the shCon group ($P < 0.05$). Treatment with AS-IV or TMP partially restored the expression of these proteins even under conditions of MALAT1 silencing. Notably, the combined treatment (shMALAT1 + AS-IV + TMP) resulted in a significantly more pronounced upregulation compared to either monotherapy ($P < 0.01$). These findings are consistent with the hypothesis that AS-IV and TMP exert an enhanced combined effect in promoting the expression of angiogenic and vascular stability markers. This effect appears to be partially mediated by the upregulation of MALAT1 and the subsequent activation of downstream targets, including CXCR4, VEGFA, Ang1, and Ang2 (**Figure 5B**).

Immunofluorescence Results Under MALAT1 Silencing

In the MALAT1 knockdown model, the immunofluorescence intensity of CXCL12, CXCR4, Ang1, and Ang2 was significantly downregulated compared to the shCon group, indicating that MALAT1 positively influences both the CXCL12/CXCR4 axis and the Ang1/Ang2 balance. Following drug treatment, AS-IV or TMP partially restored the expression of these proteins even in the presence of MALAT1 deficiency. Notably, the combined treatment (shMALAT1 + AS-IV + TMP) resulted in a significantly more pronounced recovery compared to either monotherapy ($P < 0.001$). These findings are consistent with the hypothesis that MALAT1 acts as a key regulatory factor associated with the pro-angiogenic and vascular repair effects of AS-IV and TMP, although the partial rescue suggests that additional pathways may also contribute to the observed benefits of the combination therapy (**Figure 5C**).

Discussion

In our Ischemic stroke remains one of the leading causes of disability and mortality worldwide, and the development of effective therapeutic strategies to promote vascular regeneration and repair of the neurovascular unit is of great clinical importance. The neuroprotective effects of the active components of traditional Chinese medicine, such as AS-IV and TMP, have been extensively reported in models of cerebral infarction. AS-IV has demonstrated significant neuroprotective properties in various animal models of cerebral ischemia, exerting its effects through multiple mechanisms, including antioxidative, anti-inflammatory, and anti-apoptotic pathways, ultimately reducing brain tissue damage and improving neurological function [23]. Its mechanisms of action have been shown to involve regulation of the JAK2/STAT3 signaling pathway, enhancement of mitochondrial function, activation of PINK1/Parkin-mediated mitophagy, and inhibition of CaSR-induced neuronal apoptosis [24-26]. In addition, AS-IV promotes endothelial cell proliferation and neovascularization [18], and has been shown to exert immunomodulatory effects by inhibiting histone deacetylase activity and modulating natural killer cell infiltration and cytokine expression [25].TMP, a widely used clinical vasodilator for cerebrovascular diseases, also exhibits broad neurovascular protective effects. Studies have shown that TMP can attenuate ischemia-induced neuronal damage by enhancing axonal plasticity and synaptic remodeling, promoting neurovascular unit repair, improving microcirculatory function, and activating the FGF2/PI3K/Akt signaling pathway [27,28]. Furthermore, TMP has been demonstrated to reduce BBB permeability, alleviate neuroinflammation, and inhibit the NogoA/RhoA/ROCK signaling pathway, thereby contributing to the improvement of motor function recovery [29,30]. study, AS-IV and TMP, particularly in combination, produced a more pronounced protective effect in bEnd.3 cells subjected to OGD/R. The combination significantly enhanced cell viability, migration, and the expression of angiogenesis-related proteins. While AS-IV or TMP alone partially mitigated OGD/R-induced damage, their combined application yielded superior efficacy compared to either monotherapy, demonstrating an enhanced combined effect. These findings are in line with previous reports that emphasize the neurovascular benefits of

This work is licensed under Creative Commons Attribution-NonCommercial-NoDerivatives 4.0 International (CC BY-NC-ND 4.0)

Indexed in: [Current Contents/Clinical Medicine] [SCI Expanded] [ISI Alerting System] [ISI Journals Master List] [Index Medicus/MEDLINE] [EMBASE/Excerpta Medica] [Chemical Abstracts/CAS]

these compounds, further supporting their potential in treating ischemic stroke-related endothelial dysfunction [31,32].

At the molecular level, our results highlight the MALAT1–CXCL12/CXCR4 signaling axis as a potential central pathway mediating the observed effects. MALAT1 is a long non-coding RNA known to regulate endothelial proliferation, migration, and angiogenesis. Previous studies have shown that silencing MALAT1 significantly inhibits endothelial cell functions and downregulates the expression of angiogenesis-related factors [33,34]. Furthermore, the CXCL12/CXCR4 axis is a critical chemotactic pathway that facilitates the recruitment of endothelial cells and the formation of new blood vessels independent of the classical VEGF pathway [35]. In this study, qPCR and western blot analyses revealed that OGD/R treatment significantly downregulated the expression of MALAT1. This was accompanied by a compensatory upregulation of CXCR4 and VEGFA protein levels, alongside the downregulation of Ang1 and upregulation of Ang2. These alterations suggest that OGD/R induces a profound dysregulation of the neurovascular unit, thereby compromising microvascular stability. Notably, intervention with AS-IV and TMP, particularly in combination, significantly reversed these molecular disturbances. The combination yielded a more pronounced effect than either monotherapy, suggesting an enhanced combined effect in restoring the balance of angiogenesis-related factors and activating the CXCL12/CXCR4 signaling axis in this in vitro model.

Notably, the pathophysiological cascade of cerebral ischemia-reperfusion injury involves highly interconnected networks, where endothelial dysregulation often coexists with controlled cell death pathways. Emerging evidence suggests that ferroptosis, an iron-dependent form of regulated cell death driven by lipid peroxidation, plays a critical role in microvascular damage and blood–brain barrier disruption after stroke. Recent studies have demonstrated that AS-IV can mitigate cerebral ischemia-reperfusion injury by inhibiting the P62/Keap1/Nrf2 pathway-mediated ferroptosis [36], while TMP has also been shown to attenuate ischemic damage by suppressing ferroptosis via the AMPK/Nrf2 signaling pathways [37].

Although our current study primarily delineates the regulatory effects of the AS-IV and TMP combination through the lens of the MALAT1–CXCL12/CXCR4 angiogenesis axis, the cross-talk between lncRNA-mediated endothelial repair and the inhibition of ferroptosis warrants further investigation. Given that Nrf2 activation plays a pivotal role in maintaining mitochondrial quality control and mitigating oxidative stress—both of which are critical upstream events influencing MALAT1 expression—it is highly plausible that the enhanced combined effect of AS-IV and TMP observed in this study can be partially attributed to a coordinated regulation involving both pro-angiogenic pathways and Nrf2-mediated ferroptosis resistance. Future studies utilizing pathway-specific inhibitors are required to fully elucidate this potential molecular interplay within the neurovascular unit.

Immunofluorescence results were consistent with western blot findings, further confirming the regulatory effects of the drug interventions. Specifically, Ang1 expression was markedly reduced following OGD/R treatment, suggesting that ischemia-reperfusion injury can impair vascular structural integrity and functional stability. Treatment with either AS-IV or TMP alone partially restored Ang1 expression, while the combined treatment group exhibited a significantly more pronounced upregulation compared to either monotherapy, demonstrating an enhanced combined effect in promoting the expression of vascular stabilizing factors. Conversely, Ang2 expression was significantly higher in the OGD/R group, potentially contributing to vascular instability and endothelial injury. Drug interventions downregulated Ang2 expression, with the combination therapy showing the most substantial reduction, suggesting that the combination can improve the ischemic microenvironment by inhibiting factors associated with vascular regression. Regarding the CXCL12/CXCR4 axis, both markers showed a slight increase in expression after OGD/R treatment, indicating a possible compensatory endogenous stress response. Although AS-IV or TMP monotherapy showed an upward trend in expression, these changes did not reach statistical significance. Notably, the combined treatment significantly elevated CXCL12 and CXCR4 levels, supporting the hypothesis that this drug combination can promote angiogenesis-related processes by activating the MALAT1–CXCL12/CXCR4 signaling axis in this in vitro model.

Previous studies have demonstrated that in a co-culture model of neural stem cells and microglia, MALAT1 regulates CXCR4 expression and influences the secretion of CXCL12 [38]. To further validate the regulatory role of MALAT1 in the intervention effects of AS-IV and TMP, they established a stable MALAT1-silenced cell model via lentiviral-mediated shRNA transduction. The results showed that MALAT1 silencing significantly attenuated, but did not completely abolish, the promotive effects of AS-IV and TMP on cell viability and migration. Moreover, it suppressed the expression of CXCL12 and CXCR4, and downregulated angiogenesis-related proteins, including VEGFA, Ang1, and Ang2. These findings suggest that activation of the CXCL12/CXCR4 pathway by AS-IV and TMP is at least partially dependent on the presence of MALAT1.

Immunofluorescence staining results supported this molecular mechanism, revealing that the expression levels of CXCL12, CXCR4, Ang1, and Ang2 were markedly reduced in the MALAT1-silenced model. This indicates that MALAT1 positively regulates the CXCL12/CXCR4 pathway and the expression of Ang1 and Ang2 in bEnd.3 cells. Following drug intervention, AS-IV

APPROVED GALLEY PROOF

This work is licensed under Creative Commons Attribution-NonCommercial-NoDerivatives 4.0 International (CC BY-NC-ND 4.0)

Indexed in: [Current Contents/Clinical Medicine] [SCI Expanded] [ISI Alerting System] [ISI Journals Master List] [Index Medicus/MEDLINE] [EMBASE/Excerpta Medica] [Chemical Abstracts/CAS]

APPROVED GALLEY PROOF

or TMP partially restored the expression of these molecules. Notably, the combined treatment group showed a significantly more pronounced recovery compared to either monotherapy, demonstrating an enhanced combined effect. These results further support MALAT1 as a crucial upstream regulator associated with the vascular repair effects of AS-IV and TMP, potentially through the activation of the CXCL12/CXCR4 signaling pathway to promote angiogenesis-related processes in this in vitro model.

Notably, Ang2 expression exhibited an upregulation trend in the OGD/R model, reflecting vascular stress and inflammatory responses induced by ischemia-reperfusion injury. In contrast, Ang2 expression was downregulated in the MALAT1-silenced model, suggesting a positive regulatory role of MALAT1 on Ang2. The differing expression patterns of Ang2 between the 2 models indicate that the OGD/R-induced increase in Ang2 is primarily driven by pathological stimuli, whereas the downregulation of Ang2 following MALAT1 depletion highlights its critical role at the transcriptional regulatory level. These findings suggest that Ang2 expression is subject to complex regulation by both pathological stimuli and specific transcriptional control mechanisms.

In summary, our study demonstrates the enhanced protective effects of AS-IV and TMP combination on cerebral microvascular endothelial cells in the OGD/R model. The combination alleviates ischemia-reperfusion injury by promoting cell viability, migration, and the expression of angiogenesis-related factors. Further mechanistic investigations revealed that MALAT1 plays a regulatory role in this process, contributing to the pro-angiogenic and vascular repair effects of AS-IV and TMP, likely associated with activation of the CXCL12/CXCR4 signaling pathway. While our results are consistent with the involvement of the MALAT1-mediated CXCL12/CXCR4 axis, the necessity of this pathway requires further validation using specific inhibitors or downstream gene-silencing approaches.

This study has several limitations. First, the use of the bEnd.3 cell line and the OGD/R model provides a simplified in vitro environment that does not fully replicate the physiological complexity of clinical ischemic stroke. Second, while we identified the role of MALAT1, further in vivo studies using rodent models are necessary to confirm the translational potential of the AS-IV and TMP combination.

Conclusions

This study demonstrated that the active components AS-IV and TMP exert enhanced protective effects compared to either monotherapy on cerebral microvasculature in the bEnd.3 cell OGD/R model. The combination significantly promotes the proliferation, migration, and expression of angiogenesis-related proteins in brain endothelial cells. The underlying mechanism is consistent with the upregulation of MALAT1 expression, activation of the CXCL12/CXCR4 signaling pathway, and modulation of the Ang1/Ang2 balance, which collectively contribute to improved vascular stability and regenerative capacity under ischemic-like injury in vitro. These findings provide new experimental evidence supporting the potential therapeutic benefits of combined AS-IV and TMP for ischemic stroke. Furthermore, this study highlights the potential of the AS-IV and TMP combination as a candidate strategy for promoting vascular regeneration and repair, warranting further validation in in vivo models.

Disclaimer

The views expressed in this article are those of the authors and do not necessarily reflect the official policy or position of their affiliated institutions or the funding agencies.

Data Availability Statement

The original datasets supporting the conclusions of this article are available in the article/Supplementary Material. Further inquiries can be directed to the corresponding author.

Declaration of Figures' Authenticity

All figures submitted have been created by the authors who confirm that the images are original with no duplication and have not been previously published in whole or in part.

References:

1. GBD 2021 Stroke Risk Factor Collaborators. Global, regional, and national burden of stroke and its risk factors, 1990-2021: A systematic analysis for the Global Burden of Disease Study 2021. Lancet Neurol. 2024;23(10):973-1003
2. Feigin VL, Owolabi MO, World Stroke Organization-Lancet Neurology Commission Stroke Collaboration Group. Pragmatic solutions to reduce the global burden of stroke: A World Stroke Organization-Lancet Neurology Commission. Lancet Neurol. 2023;22(12):1160-206
3. Feigin VL, Brainin M, Norrving B, et al. World Stroke Organization: Global stroke fact sheet 2025. Int J Stroke. 2025;20(2):132-44
4. Beck H, Plate KH. Angiogenesis after cerebral ischemia. Acta Neuropathol. 2009;117(5):481-96
5. Hatakeyama M, Ninomiya I, Kanazawa M. Angiogenesis and neuronal remodeling after ischemic stroke. Neural Regen Res. 2020;15(1):16-19
6. Hu B, Pei J, Wan C, et al. Mechanisms of postischemic stroke angiogenesis: A multifaceted approach. J Inflamm Res. 2024;17:4625-46
7. Maguida G, Shuaib A. Collateral circulation in ischemic stroke: An updated review. J Stroke. 2023;25(2):179-98
8. Perovic T, Harms C, Gerhardt H. Formation and maintenance of the natural bypass vessels of the brain. Front Cardiovasc Med. 2022;9:778773

This work is licensed under Creative Commons Attribution-NonCommercial-NoDerivatives 4.0 International (CC BY-NC-ND 4.0)

Indexed in: [Current Contents/Clinical Medicine] [SCI Expanded] [ISI Alerting System] [ISI Journals Master List] [Index Medicus/MEDLINE] [EMBASE/Excerpta Medica] [Chemical Abstracts/CAS]

9. Faber JE. Collateral blood vessels in stroke and ischemic disease: Formation, physiology, rarefaction, remodeling. J Cereb Blood Flow Metab. 2025;45(6):1007-30
10. Lin Y, Pang Q, Shi Y, et al. Long noncoding RNA MALAT1 promotes angiogenesis through the caveolin-1/VEGF pathway after cerebral ischemic injury. Neuroreport. 2025;36(7):350-63
11. Wang Y, Huang J, Li Y, et al. Roles of chemokine CXCL12 and its receptors in ischemic stroke. Curr Drug Targets. 2012;13(2):166-72
12. Li Y, Chang S, Li W, et al. cxcl12-engineered endothelial progenitor cells enhance neurogenesis and angiogenesis after ischemic brain injury in mice. Stem Cell Res Ther. 2018;9(1):139
13. Li B, Bai W, Sun P, et al. The effect of CXCL12 on endothelial progenitor cells: Potential target for angiogenesis in intracerebral hemorrhage. J Interferon Cytokine Res. 2015;35(1):23-31
14. Chen ZZ, Gong X, Guo Q, et al. Bu Yang Huan Wu decoction prevents reperfusion injury following ischemic stroke in rats via inhibition of HIF-1 alpha, VEGF and promotion beta-ENaC expression. J Ethnopharmacol. 2019;228:70-81
15. Zhou L, Guo SN, Gao Y. Effects and perspectives of Chinese patent ,edicines for Tonifying Qi and promoting blood circulation on patients with cerebral infarction. Curr Vasc Pharmacol. 2015;13(4):475-91
16. Wang SG, Xu Y, Chen JD, et al. Astragaloside IV stimulates angiogenesis and increases nitric oxide accumulation via JAK2/STAT3 and ERK1/2 pathway. Molecules. 2013;18(10):12809-19
17. Kang X, Su S, Hong W, et al. Research progress on the ability of Astragaloside IV to protect the brain against ischemia-reperfusion injury. Front Neurosci. 2021;15:755902
18. Shi G, Chen J, Zhang C, et al. Astragaloside IV promotes cerebral angiogenesis and neurological recovery after focal ischemic stroke in mice via activating PI3K/Akt/mTOR signaling pathway. Heliyon. 2023;9(12):e22800
19. Lei X, Zhang L, Li Z, et al. Astragaloside IV/lncRNA-TUG1/TRAF5 signaling pathway participates in podocyte apoptosis of diabetic nephropathy rats. Drug Des Devel Ther. 2018;12:2785-93
20. Li L, Chen H, Shen A, et al. Ligustrazine inhibits platelet activation via suppression of the Akt pathway. Int J Mol Med. 2019;43(1):575-82
21. Ding Y, Du J, Cui F, et al. The protective effect of ligustrazine on rats with cerebral ischemia-reperfusion injury via activating PI3K/Akt pathway. Hum Exp Toxicol. 2019;38(10):1168-77
22. Deng M, Cai Y, Wang Y, et al. Tetramethylpyrazine attenuates the blood-brain barrier damage against ischemic stroke by targeting endothelin-1/Akt pathway in astrocytes. Front Pharmacol. 2025;16:1571552
23. Wang HL, Zhou QH, Xu MB, et al. Astragaloside IV for experimental focal cerebral ischemia: Preclinical evidence and possible mechanisms. Oxid Med Cell Longev. 2017;2017:8424326
24. Xu Z, Liu W, Huang H. Astragaloside IV alleviates cerebral ischemia-reperfusion injury by activating the Janus kinase 2 and signal transducer and activator of transcription 3 signaling pathway. Pharmacology. 2020;105(3-4):181-89
25. He T, Zhou X, Wang X, et al. Astragaloside IV ameliorates cerebral ischemic-reperfusion injury via improving mitochondrial function and inhibiting neuronal apoptosis. Curr Issues Mol Biol. 2025;47(8):597
26. Du SJ, Zhang Y, Zhao YM, et al. Astragaloside IV attenuates cerebral ischemia-reperfusion injury in rats through the inhibition of calcium-sensing receptor-mediated apoptosis. Int J Mol Med. 2021;47(1):302-14
27. Feng XF, Lei JF, Li MZ, et al. Magnetic resonance imaging investigation of neuroplasticity after ischemic stroke in tetramethylpyrazine-treated rats. Front Pharmacol. 2022;13:851746
28. Feng XF, Li MC, Lin ZY, et al. Tetramethylpyrazine promotes stroke recovery by inducing the restoration of neurovascular unit and transformation of A1/A2 reactive astrocytes. Front Cell Neurosci. 2023;17:1125412
29. Lin JB, Zheng CJ, Zhang X, et al. Effects of tetramethylpyrazine on functional recovery and neuronal dendritic plasticity after experimental stroke. Evid Based Complement Alternat Med. 2015;2015:394926
30. Wang A, Zhu G, Qian P, et al. Tetramethylpyrazine reduces blood-brain barrier permeability associated with enhancement of peripheral cholinergic anti-inflammatory effects for treating traumatic brain injury. Exp Ther Med. 2017;14(3):2392-400
31. Zhang R, Wu F, Cheng B, et al. Apelin-13 prevents the effects of oxygen-glucose deprivation/reperfusion on bEnd.3 cells by inhibiting AKT-mTOR signaling. Exp Biol Med (Maywood). 2023;248(2):146-56
32. Ku JM, Taher M, Chin KY, et al. Characterisation of a mouse cerebral microvascular endothelial cell line (bEnd.3) after oxygen glucose deprivation and reoxygenation. Clin Exp Pharmacol Physiol. 2016;43(8):777-86
33. Ning J, Yang R, Wang H, et al. LncRNA MALAT1 silencing represses CXCL12-induced proliferation, invasion, and homing behavior in multiple myeloma by inhibiting CXCR4. Hematology. 2024;29(1):2422154
34. Wang C, Qu Y, Suo R, et al. Long non-coding RNA MALAT1 regulates angiogenesis following oxygen-glucose deprivation/reoxygenation. J Cell Mol Med. 2019;23(4):2970-83
35. Teicher BA, Fricker SP. CXCL12 (SDF-1)/CXCR4 pathway in cancer. Clin Cancer Res. 2010;16(11):2927-31
36. Wang L, Liu C, Wang L, et al. Astragaloside IV mitigates cerebral ischaemia-reperfusion injury via inhibition of P62/Keap1/Nrf2 pathway-mediated ferroptosis. Eur J Pharmacol. 2023;944:175516
37. Zhong KX, Zeng Q, Tang H, et al. Tetramethylpyrazine attenuates cerebral ischemia-reperfusion injury by inhibiting ferroptosis via the AMPK/Nrf2 pathways. J Stroke Cerebrovasc Dis. 2025;34(2):108196
38. Dong Q, Chen P, Qiu W, et al. Long non-coding RNA Malat1 modulates CXCR4 expression to regulate the interaction between induced neural stem cells and microglia following closed head injury. Stem Cell Res Ther. 2025;16(1):31

APPROVED GALLEY PROOF

This work is licensed under Creative Commons Attribution-NonCommercial-NoDerivatives 4.0 International (CC BY-NC-ND 4.0)

Indexed in: [Current Contents/Clinical Medicine] [SCI Expanded] [ISI Alerting System] [ISI Journals Master List] [Index Medicus/MEDLINE] [EMBASE/Excerpta Medica] [Chemical Abstracts/CAS]